YALE PEABODY MUSEUM

JOURNAL OF MARINE RESEARCH

The *Journal of Marine Research,* one of the oldest journals in American marine science, published important peer-reviewed original research on a broad array of topics in physical, biological, and chemical oceanography vital to the academic oceanographic community in the long and rich tradition of the Sears Foundation for Marine Research at Yale University.

An archive of all issues from 1937 to 2021 (Volume 1–79) are available through EliScholar, a digital platform for scholarly publishing provided by Yale University Library at https://elischolar.library.yale.edu/.

Requests for permission to clear rights for use of this content should be directed to the authors, their estates, or other representatives. The *Journal of Marine Research* has no contact information beyond the affiliations listed in the published articles. We ask that you provide attribution to the *Journal of Marine Research.*

Yale University provides access to these materials for educational and research purposes only. Copyright or other proprietary rights to content contained in this document may be held by individuals or entities other than, or in addition to, Yale University. You are solely responsible for determining the ownership of the copyright, and for obtaining permission for your intended use. Yale University makes no warranty that your distribution, reproduction, or other use of these materials will not infringe the rights of third parties.

Size-fractionated ^{234}Th in continental shelf waters off New England: Implications for the role of colloids in oceanic trace metal scavenging

by S. Bradley Moran[1,2] and Ken O. Buesseler[1]

ABSTRACT

Measurements of ^{234}Th ($t_{1/2}$ = 24.1 days) in dissolved, colloidal, and particulate forms have been made to investigate the role of colloids in reactive metal scavenging in the surface waters of Buzzards Bay, over an annual cycle, and in the shelf and slope waters off New England. At-sea sampling involved prefiltering seawater through 0.2 μm filters followed by cross-flow filtration using a 10,000 nominal molecular weight filter to collect colloidal (10,000 NMW-0.2 μm) and dissolved (< 10,000 NMW) phases. Total ^{234}Th activities increase with distance from shore, indicative of enhanced scavenging in the particle-rich nearshore waters. Clearly seen in Buzzards Bay are seasonal changes in total ^{234}Th, with activities ranging from ~ 0.7 dpm l^{-1} in the winter, preceeding a phytoplankton bloom, to ~ 0.2 dpm l^{-1} in the summer. Throughout the annual cycle, 2–16% of total ^{234}Th is colloidal, 22–40% is dissolved, and 45–75% is particulate. In the offshore waters, ~ 1% of total ^{234}Th is colloidal, 2–6% is particulate, and 93–98% is dissolved. The ^{234}Th size-distribution exhibits a systematic increase in the association of ^{234}Th with particulate and, to a lesser extent, colloidal matter with increasing suspended particle concentration (C_p). Moreover, a first-order prediction of the fractionation of ^{234}Th between the various size classes is demonstrated using measured solid-solution partition coefficients. Box model calculations indicate a mean residence time of colloidal ^{234}Th with respect to aggregation into particles of 0.3 days in Buzzards Bay, which compares with 2 days for dissolved and 4 days for particulate ^{234}Th. In the offshore surface waters, colloidal and particulate ^{234}Th residence times are ~ 0.5 days and 2–3 days respectively, compared with 30–85 days for the dissolved phase. The short and relatively invariant residence time of colloidal ^{234}Th suggests that colloidal aggregation may not be rate-limiting in controlling the scavenging of thorium and, by analogy, other particle-reactive trace metals. An implication of these results is that colloidal ^{234}Th may be tracing a reactive intermediate in the bacterially mediated decomposition of large, rapidly-sinking biogenic aggregates. Using the size-fractionated ^{234}Th data, we demonstrate that K_d values for thorium are invariant with C_p and that scavenging rate constants exhibit a first-order dependence on C_p. Thus, "particle-concentration effects" are negligible for oceanic waters (C_p ~ 0.01–1 mg l^{-1}).

1. Department of Marine Chemistry and Geochemistry, Woods Hole Oceanographic Institution, Woods Hole, Massachusetts, 02543, U.S.A.
2. Present address: The University of Rhode Island, Graduate School of Oceanography, Narragansett, Rhode Island, 02882-1197, U.S.A.

1. Introduction

Oceanic particulate matter plays an important role in the sorptive removal of reactive chemicals, inorganic and organic, from seawater and in rapidly transporting organic matter and associated elements to the sediments. Studies of this removal process, referred to as "scavenging" (Goldberg, 1954), have traditionally been conducted using filters of 0.2–1 μm pore size to define dissolved and particulate species. An important caveat of this operational size definition is that submicron colloidal matter (~0.001–1 μm; Stumm, 1977) is included in the "dissolved" (<0.2–1 μm) phase. Although measurements of the colloidal size range have rarely been reported, evidence is accumulating to suggest that colloids may play a role in marine scavenging (Honeyman and Santschi, 1989, 1991; Moran and Moore, 1989, 1992; Moran and Buesseler, 1992; Baskaran *et al.*, 1992).

Several recent studies have provided new evidence for the importance of colloids in ocean biogeochemistry. High concentrations (up to 10^8 ml^{-1}) of nonliving, submicron (0.38–1 μm) particles have been reported in the surface waters of the North Pacific (Koike *et al.*, 1990) and in coastal waters off Nova Scotia, Canada (Longhurst *et al.*, 1992). Wells and Goldberg (1991) extended the size range of these abundant colloids down to ~5 nm in the surface waters off California. These observations provide direct evidence that a significant fraction of "dissolved" organic matter (DOM) and hence organic carbon in the oceans exists in the colloidal size range. Indeed, Benner *et al.* (1992) reported that 22–33% of "dissolved" (<0.2 μm) organic carbon is in the 1,000 NMW-0.2 μm size range in North Pacific surface waters. Moreover, these authors suggested that macromolecular components of DOM are reactive, largely composed of polysaccharides, and may support much of the heterotrophic activity in the surface ocean. The suggested reactive nature of this material is consistent with the short residence time of colloidal ^{234}Th reported in the surface waters near Bermuda (Moran and Buesseler, 1992) and in the Gulf of Mexico (Baskaran *et al.*, 1992). The implication of these recent studies is that colloids may play an important role in oceanic trace metal scavenging and particle cycling.

Thorium isotopes (^{234}Th, ^{228}Th, and ^{230}Th), due to their strong chemical reactivity for marine particle surfaces and *in-situ* radiogenic source (^{238}U, ^{228}Ra, and ^{234}U, respectively), are useful tracers for studying trace metal scavenging and particle dynamics in the oceans (e.g. Bacon and Anderson, 1982; Nozaki *et al.*, 1981, 1987; Coale and Bruland, 1985, 1987). Rates of scavenging can be quantified by measuring the disequilibrium between the parent and daughter nuclides that results from the removal of thorium from the water column on suspended and sinking particulate matter. Thorium-234, with a half-life of 24.1 days, is an excellent tracer for quantifying rates of dissolved metal-particle interactions on time-scales of 1–100 days (e.g. Coale and Bruland, 1985, 1987; Buesseler *et al.*, 1992a; Moran and Buesseler, 1992), which correspond to rates of biogenic processes occurring in the upper ocean.

In this study, we used ^{234}Th as a tracer to investigate the role of colloids in oceanic
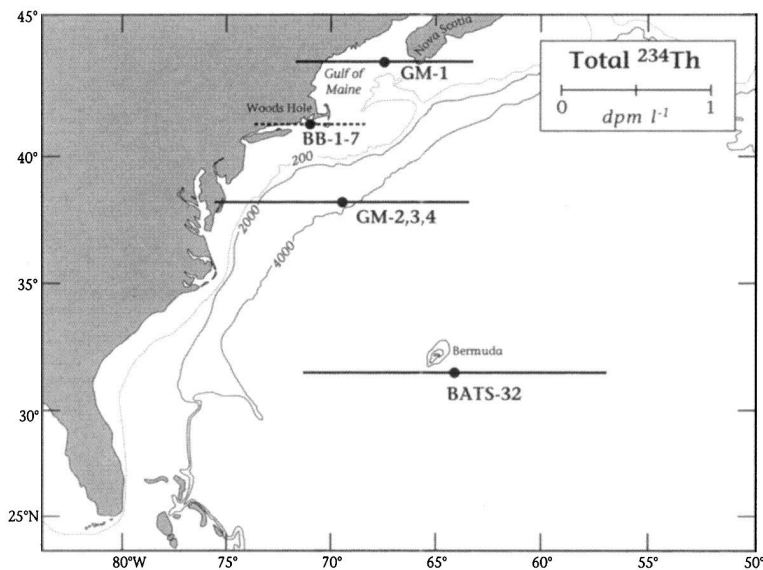
Figure 1. Map showing sampling stations (●) occupied in Buzzards Bay, BB-1-7 (water depth 10 m), and on the Gulf of Maine cruise, GM-1 (water depth 251 m) and GM-2, 3, 4 (water depth 3660 m). Total ^{234}Th activities (dpm l^{-1}) in the surface waters are proportional to the length of the line shown in the legend. Seasonal range in total ^{234}Th in Buzzards Bay indicated by dashed line. Data near Bermuda (BATS-32) from Moran and Buesseler (1992).

trace metal scavenging. Our primary aim was to quantify the temporal and spatial scales of variability of colloidal ^{234}Th (10,000 NMW-0.2 μm) in continental shelf waters off New England. The strategy was to collect samples over a range in suspended particle concentration and hence total ^{234}Th activity, which in turn is reflected in the size-distribution of ^{234}Th. Estimates of the temporal and spatial variability in ^{234}Th residence times in the various size classes are made using a simple box model. In addition, we use the size-fractionated data to examine the effect of colloids on the solid-solution partition coefficients (K_d's) and scavenging rate constants (k'_1) of thorium as a function of particle concentration.

2. Materials and methods

a. Sampling. Seawater samples were collected at a single site in Buzzards Bay (BB-1-7), MA, from June 24, 1991, to July 28, 1992, and during a cruise to the Gulf of Maine (GM-1,2,3,4), July 17–30, 1991 (Fig. 1, Table 1). In Buzzards Bay, a peristaltic pump was used to pump seawater (~50–70 liters) from a depth of 2 meters through acid-cleaned Bevaline tubing and acid-cleaned 0.2 μm Gelman Mini-Capsule filters (filtration area 500 cm^2). Prefiltered (<0.2 μm) seawater was collected in a Millipore Pellicon cross-flow filtration system (described below). During the Gulf of Maine

Table 1. Sampling dates, locations, and ancillary data for Buzzards Bay and the Gulf of Maine cruise.

Sample Code	Date	Latitude (N)	Longitude (W)	Depth (m)	Salinity (psu)	Temp. (°C)	NO_3 (μmol l^{-1})	PO_4 (μmol l^{-1})	SiO_2 (μmol l^{-1})	Bacteria (10^6 ml^{-1})	Chl. a (μg l^{-1})	POC (μmol l^{-1})	C_p (mg l^{-1})
BB-1	6/25/91	41°32.80'	70°46.12'	2	31.686	19.4	0.47	0.57	9.84	4.0	0.52	25.3	0.96
BB-2	10/22/91	41°32.80'	70°46.12'	2	31.771	15.0	0.43	0.70	0.55	1.4	0.82	23.8	1.80
BB-3	11/19/91	41°32.80'	70°46.12'	2	31.544	9.1	1.03	0.85	3.94	1.6	1.00	30.9	1.42
BB-4	1/3/92	41°32.80'	70°46.12'	2	31.245	4.0	0.90	0.72	0.86	0.4	0.51	34.6	1.26
BB-5	2/7/92	41°32.80'	70°46.12'	2	31.570	4.0	0.28	0.77	0.72	0.8	2.50	47.2	2.61
BB-6	3/31/92	41°32.80'	70°46.12'	2	31.480	3.9	0.24	0.66	0.16	0.4	0.42	10.9	0.48
BB-7	7/28/92	41°32.80'	70°46.12'	2	31.468	13.0	0.20	0.36	7.08	2.8	0.85	26.1	0.88
GM-1	7/21/91	43°34.09'	67°51.17'	15	32.165	8.0	—	—	—	—	—	—	0.10*
GM-2	7/25/91	38°18.03'	69°35.26'	3552	34.900	3.5	—	—	—	—	—	—	0.01*
GM-3	7/26/91	38°19.47'	69°33.41'	2000	34.891	3.5	—	—	—	—	—	—	0.01*
GM-4	7/26/91	38°17.04'	69°36.00'	15	31.771	7.2	—	—	—	—	—	—	0.05*

BB = Buzzards Bay.

GM = Gulf of Maine cruise.

* = Estimated C_p.

cruise, approximately 100 liters of seawater were collected at each station using 30 liter Go-Flo bottles. Seawater was prefiltered through 0.2 μm Gelman Mini-Capsule filters using a peristaltic pump and the filtrate collected in the cross-flow filtration system.

In order to calculate a mass balance, separate unfiltered samples were collected at all stations for determination of total [234]Th. Subsamples of the traditionally defined "dissolved" (<0.2 μm) phase were also collected.

b. Cross-flow filtration. A Millipore Pellicon cross-flow filtration (CFF) system modified for trace metal sampling was used to collect dissolved (in this work: <10,000 nominal molecular weight, NMW) and colloidal (10,000 NMW-0.2 μm) samples. Details of the design and operation of the modified CFF system are described in Moran (1991). The sustained high flow rates (10–25 liters hr^{-1} in this study) of CFF facilitated the collection within several hours of the large sample volumes (50–100 liters) required for the determination of size-fractionated [234]Th.

The CFF system was fitted with a 10,000 NMW filter (~1–10 nm pore size; 0.464 m^2 filtration area) made of regenerated cellulose, which is reported to have reduced protein binding characteristics (Millipore Corp.). The CFF system was initially cleaned in the lab by soaking for ~48 hours in 2 M HCl and then thoroughly rinsed with Milli-Q water (Moran, 1991). Cross-flow filtration of all samples was conducted at sea and completed within 3–6 hours of sample collection. Immediately following prefiltration, the CFF system was rinsed by pumping 2–3 liters of prefiltered sample through the system with the permeate and retentate lines going to waste. The CFF filter was then preconditioned by soaking the filter in prefiltered seawater sample for 15–30 minutes. Preconditioning reduces the retention of solutes onto the filter (polarization) and adsorptive losses of thorium (Niven and Moore, 1988; Moran, 1991). Samples were then cross-flow filtered in the concentrate mode, resulting in the separation of the dissolved phase and the concentration of the colloidal phase (Moran, 1991). No significant decreases in filtration rate were observed during cross-flow filtration that would indicate clogging of the CFF filter. Final sample volumes in the CFF reservoir were typically 5–10 liters, resulting in volume concentration factors of 6–10 for Buzzards Bay samples and 10–25 for the Gulf of Maine cruise samples. After processing each sample, the CFF filter was leached for 15–20 minutes with 1 M HCl to determine any sorptive loss of [234]Th. When not in use, the CFF filter was cleaned with 1 M HCl, rinsed with Milli-Q water, and stored in dilute (~0.01 M) HCl.

Total, dissolved, colloidal, "dissolved" (<0.2 μm), particulate (>0.2 μm) and acid-leach samples were transported to WHOI for [234]Th determination.

*c. *[234]*Th determination.* To each of the total, dissolved, colloidal and acid-leach samples were added ~30 ml of concentrated HNO_3, ~7 dpm of [230]Th yield monitor,

and 5 ml of 50 mg ml^{-1} FeCl$_3$ carrier (cf Anderson and Fleer, 1982; Fleer and Bacon, 1991). Samples were stirred for $\sim$24 hours at room temperature to equilibrate the yield monitor and Fe with the sample. The pH was increased to $\sim$8 with NH$_4$OH and the Fe precipitate containing Th and U isotopes was allowed to settle for $\sim$12 hours. The supernatant was drawn off and the precipitate collected by centrifugation. The precipitate was washed with pH 8 Milli-Q water to remove salts, centrifuged, and the precipitate dissolved in 40 ml of 8 M HCl. Thorium-234 was separated from ^{238}U by passing the Fe solution through an anion exchange column (10 ml of AG 1-X8, 100–200 mesh) conditioned with 8 M HCl. The eluant and column rinses containing ^{234}Th were heated to dryness and taken up in 20 ml of 8 M HNO$_3$. Thorium-234 was further purified of ^{238}U by passing the solution through an anion exchange column (10 ml of AG 1-X8, 100–200 mesh) conditioned with 8 M HNO$_3$. Thorium was eluted with 8 M HCl and the eluant evaporated to dryness in the presence of concentrated H$_2$SO$_4$ and held for electroplating.

Particulate ^{234}Th was determined by combusting the Gelman filters at 500°C for 12–14 hours. Approximately 300 ml of 8 M HNO$_3$ and 7 dpm of ^{230}Th yield monitor were added to the ash and heated for $\sim$24 hours. The sample was cooled and filtered through a glass fiber filter (Whatman GF/F). To digest residual organic matter, 30% H$_2$O$_2$ was added dropwise to the filtrate while heating gently until effervescence stopped. The solution ($\sim$100 ml) was passed through an anion exchange column (25 ml of Ag 1-X8, 50–100 mesh) conditioned with 8 M HNO$_3$. ^{234}Th was further purified of ^{238}U using 8 M HCl and 8 M HNO$_3$ conditioned columns as described above and then held for electroplating.

In preparation for electroplating, samples were taken up in 5 ml of deionized water plus 10 drops of 14 M NH$_4$OH and the solution neutralized with 18 M H$_2$SO$_4$. The solution was transferred to a plating cell and the pH adjusted to 2–3 using 2 M NH$_4$OH. Thorium was electroplated onto stainless steel planchets for 2 hours with a 1 amp current at $\sim$10 volts. Planchets were rinsed with deionized water and acetone, mounted on acrylic cards, and covered with aluminum foil (9 mg cm^{-2}) to absorb low energy beta emissions. Low background (0.4–0.5 cpm), anticoincidence, gas-flow beta detectors were used to count samples once per week for 4–5 weeks. The ^{234}Th activity was quantified by counting the stronger beta emissions of its daughter ^{234m}Pa ($E = 2.29$ MeV, $t_{1/2} = 1.2$ min.). Beta detectors were calibrated using deep ocean samples in which ^{234}Th is in secular equilibrium with ^{238}U. Uranium-238 activities (dpm l^{-1}) were calculated from salinity using the relationship ^{238}U $= 0.07097 \times$ salinity @ 35 psu (Chen *et al.*, 1986). Thorium-230 yield monitor was determined by alpha counting using silicon surface barrier detectors. Thorium-234 activities (dpm l^{-1}) were corrected for ingrowth from ^{238}U, chemical yield, and decay-corrected to the mid-point of sample collection. Errors in the ^{234}Th data were propagated from counting statistics, based upon the fit of the raw counts to the ^{234}Th decay curve.

Total ^{234}Th activities were determined in three surface water samples (BB-1,

GM-1 and GM-4) by large-volume ($\sim$ 500–1000 liters) pumping through MnO_2 impregnated cartridges and gamma counting (Buesseler *et al.*, 1992b). Cartridges were ashed at 500°C overnight and the 63.3 keV energy of the ash counted using a pure Ge detector.

d. Ancillary measurements. Samples for chlorophyll *a* and particulate organic carbon (POC) analysis were collected using precombusted glass fiber filters (Whatman GF/F). Chlorophyll *a* concentrations were determined by extraction in 90% acetone and measuring the fluorescence using a Turner fluorometer (Strickland and Parsons, 1972). POC concentrations were quantified using a Perkin Elmer CHN autoanalyzer. Bacterial counts on unfiltered and 0.2 μm filtered seawater samples were made using the acridine orange method (Watson *et al.*, 1977). Reactive phosphate, silicate, and nitrate concentrations were determined using standard colorimetric methods (Strickland and Parsons, 1972) in filtered (0.2 μm) samples. The concentration of suspended particulate matter (C_p) was determined using preweighed 0.2 μm, 142-mm diameter, Poretics filters. Salinities were determined on stored samples at WHOI using a Guildline Autosal. *In-situ* seawater temperature was measured using a thermometer in Buzzards Bay and a CTD on the Gulf of Maine cruise.

3. Results

a. ^{234}Th mass balance. The ^{234}Th mass balance results are illustrated in Figure 2. Total ^{234}Th in unfiltered samples are, with the exception of two samples, within 5–10% of the sum of the dissolved, colloidal, and particulate activities. As an independent check, the sum of "dissolved" (<0.2 μm) (which should equal the dissolved plus colloidal fractions) and particulate activities also agree well with total ^{234}Th (Fig. 2). These results indicate that losses of ^{234}Th to the CFF system were minor and are consistent with the low (often undetectable) activities (<2% of total) determined in the acid-leach samples. By comparison, Baskaran *et al.* (1992) reported ^{234}Th losses to their Amicon CFF system ranging from <20% in 9 of 14 samples to 23–49% of the total for the remaining samples. The higher losses reported in the Gulf of Mexico study may be due to higher water temperatures (20–30°C; mean = 27°C; P. Santschi, personal communication), longer cross-flow filtration times (7–12 hours) or, possibly, to differences in the CFF system (polysulfone membrane compared with regenerated cellulose used in this study).

b. Seasonal changes in total ^{234}Th and biological activity in Buzzards Bay. The annual cycle of total ^{234}Th is characterized by lower activities in the spring and summer (0.1–0.2 dpm l^{-1}) than in winter (0.6–0.7 dpm l^{-1}) (Fig. 3, Table 2). Total ^{234}Th activities follow chlorophyll *a*, particulate organic carbon, and suspended particle (C_p) concentrations. Bacteria numbers range from 0.4–4.0 × 10^6 ml^{-1} and correlate to some degree with temperature ($r^2 = 0.79$, $n = 7$). Bacteria were essentially
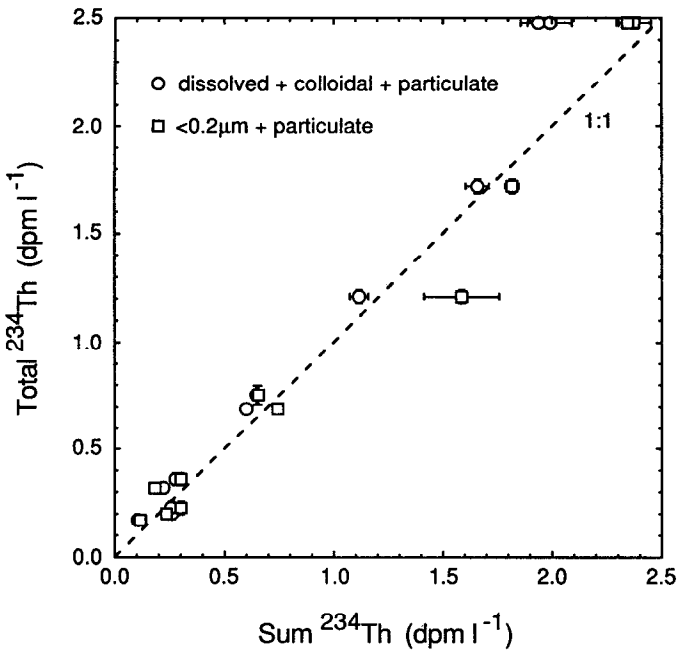
Figure 2. Mass balance results for samples of size-fractionated ^{234}Th from Buzzards Bay and the Gulf of Maine cruise. Total ^{234}Th activities were measured in separate, unfiltered samples. Sum ^{234}Th represents ($\bigcirc$) the sum of dissolved, colloidal and particulate ^{234}Th and ($\square$) the sum of "dissolved" (< 0.2 μm) and particulate ^{234}Th.

undetectable ($< 1 \times 10^4$ ml^{-1}) in the 0.2 μm filtrates, indicating that bacteria were excluded from the 10,000 NMW-0.2 μm colloidal samples. Temporal changes in nutrients are characterized by high levels of nitrate in the winter, elevated silicate concentrations in the summer, and relatively invariant phosphate levels. Total ^{234}Th increased from fall to winter, reaching a maximum (~ 0.7 dpm l^{-1}) in February, 1992. A winter phytoplankton bloom is evident at this time, when chlorophyll *a*, POC, and C_p concentrations were maximum and coincident with a marked decrease in nitrate. The timing of the bloom is consistent with previous studies of phytoplankton in this region (Glibert *et al.*, 1982, 1985). Following the bloom, total ^{234}Th decreased to a minimum in the spring, followed by a slight increase in the summer.

c. Size-fractionated ^{234}Th. Seasonal changes in dissolved, colloidal and particulate ^{234}Th activities in Buzzards Bay are shown in Figure 4 and listed in Table 2. Colloidal activities are low (0.01–0.04 dpm l^{-1}) and follow the temporal changes evident in dissolved and particulate ^{234}Th. Particulate activities are highest, ranging from 0.05 to 0.4 dpm l^{-1} . As a percentage of the total activity (Fig. 5a), colloidal ^{234}Th was highest during the spring and summer (10–16%) compared with the winter (2–5%). The fraction of what is typically defined as "dissolved" (i.e. < 0.2 μm) that is
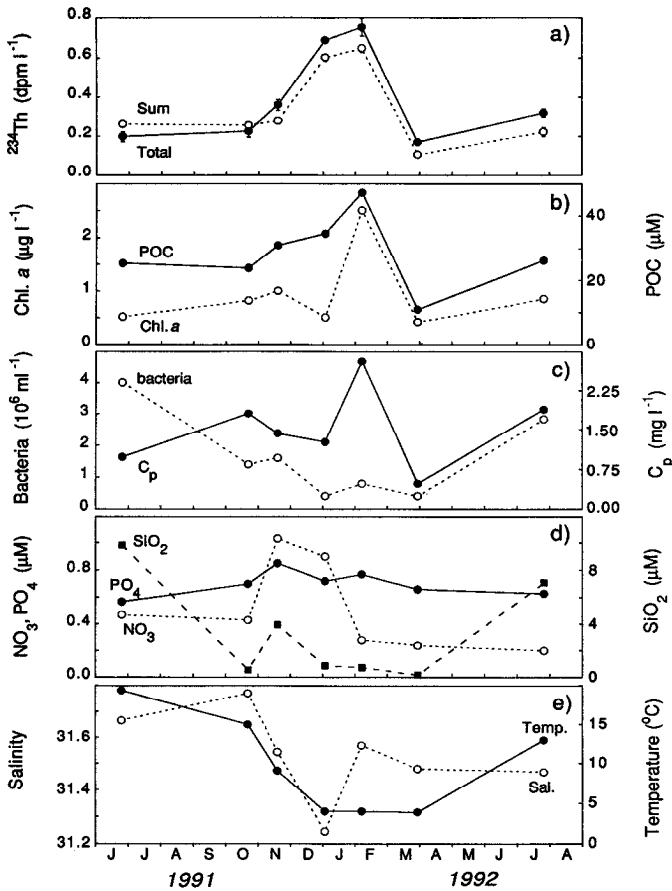
Figure 3. Seasonal changes in total ^{234}Th, chlorophyll *a*, particulate organic carbon (POC), bacteria, suspended particle concentration (C_p), nutrients, salinity, and temperature in the surface waters (2 m) of Buzzards Bay. Shown in the plot of total ^{234}Th are measurements of ^{234}Th in (●) unfiltered samples and (○) the sum of dissolved, colloidal, and particulate activities.

colloidal ranges from 5–29% of total ^{234}Th. The dissolved fraction ranges from 22% to 40%, with a higher percentage observed in the spring and summer. The particulate phase represented the majority (45–75%) of the total activity throughout the year and, unlike the dissolved and colloidal fractions, was a higher percentage during the winter.

In the shelf and slope waters, where total ^{234}Th activities are higher (Fig. 1), the size-fractionated results are characterized by high dissolved ^{234}Th compared with colloidal and particulate activities (Table 2). As a percentage of the total activity (Fig. 5b), colloidal ^{234}Th activities range from ~1% (0.01 to 0.02 dpm l^{-1}) in the surface waters to <1% (0.001 dpm l^{-1}) in the deep waters (2000 m and 3552 m).

Table 2. Size-fractionated and total ^{234}Th activities (dpm l^{-1}). ^{238}U activities calculated from salinity.

Sample Code	Dissolved (<10⁴ NMW)	Colloidal (10⁴ NMW-0.2 μm)	"Dissolved"* (<0.2 μm)	Particulate (>0.2 μm)	Sum** Fractions	Total***	^{238}U‡
BB-1	0.103 ± 0.003	0.041 ± 0.005	0.119 ± 0.023	0.118 ± 0.005	0.263 ± 0.007	0.199 ± 0.025	2.241
BB-2	0.057 ± 0.004	0.007 ± 0.006	0.109 ± 0.009	0.194 ± 0.010	0.258 ± 0.013	0.227 ± 0.031	2.248
BB-3	0.085 ± 0.007	0.015 ± 0.007	0.123 ± 0.010	0.179 ± 0.001	0.279 ± 0.010	0.360 ± 0.028	2.231
BB-4	0.206 ± 0.012	0.012 ± 0.012	0.362 ± 0.014	0.385 ± 0.006	0.602 ± 0.018	0.689 ± 0.014	2.209
BB-5	0.211 ± 0.007	0.033 ± 0.007	0.254 ± 0.008	0.404 ± 0.016	0.648 ± 0.019	0.754 ± 0.044	2.233
BB-6	0.042 ± 0.004	0.015 ± 0.005	0.068 ± 0.004	0.049 ± 0.005	0.106 ± 0.008	0.170 ± 0.006	2.227
BB-7	0.090 ± 0.015	0.023 ± 0.016	0.074 ± 0.005	0.110 ± 0.008	0.223 ± 0.023	0.319 ± 0.021	2.226
GM-1	1.039 ± 0.030	0.017 ± 0.030	1.524 ± 0.169	0.064 ± 0.006	1.119 ± 0.042	1.209 ± 0.030	2.277
GM-2	1.849 ± 0.057	0.001 ± 0.057	2.285 ± 0.076	0.088 ± 0.010	1.938 ± 0.081	2.477†	2.477
GM-3	1.946 ± 0.070	0.001 ± 0.071	2.301 ± 0.035	0.044 ± 0.018	1.991 ± 0.101	2.476†	2.476
GM-4	1.599 ± 0.030	0.010 ± 0.040	1.768 ± 0.022	0.050 ± 0.018	1.660 ± 0.053	1.715 ± 0.033	2.248

*"Dissolved" is the fraction passing through a 0.2 μm Gelman filter.
**Sum Fractions = dissolved + colloidal + particulate.
***Total = ^{234}Th determined on separate, unfiltered sample.
†Total ^{234}Th calculated from salinity for these two deep ocean samples.
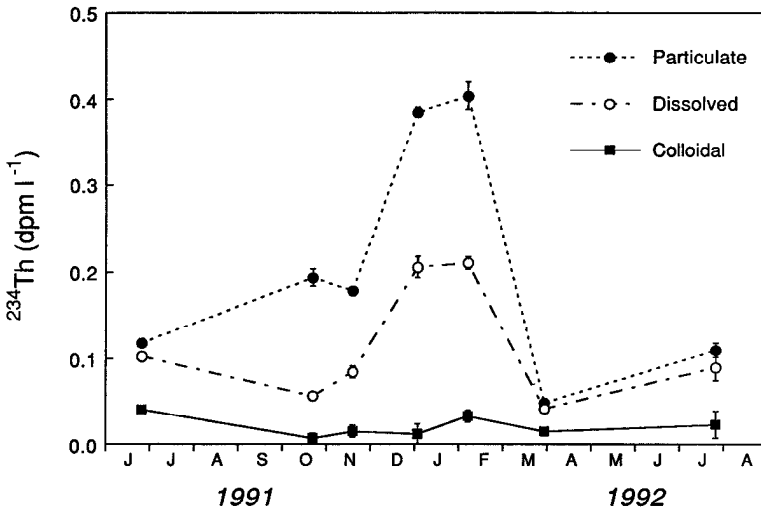‡^{238}U = 0.07097 × salinity @ 35 psu (Chen et al., 1986).

Figure 4. Seasonal changes in dissolved, colloidal, and particulate ^{234}Th in Buzzards Bay
surface waters.

Dissolved values range from 93–96% (1.04–1.60 dpm l^{-1}) in the surface waters to
95–98% (1.85–1.95 dpm l^{-1}) of the total in the deep waters. Particulate ^{234}Th is
slightly higher than the colloidal fraction, ranging from ~3–6% of the total (0.05–
0.06 dpm l^{-1}) in the surface waters to ~2–4% (0.04–0.09 dpm l^{-1}) in the deep waters.

d. ^{234}*Th partition coefficients.* Coefficients for the partitioning of ^{234}Th between the
dissolved and particulate phase (K_p), the dissolved and colloidal phase (K_c) and the
traditionally defined "dissolved" (<0.2 μm) and particulate phase (K_d) are listed in
Table 3 (Eqs. B1–B3, Appendix B). Values for K_p are fairly constant
(1.7 ± 1.2 × 10^6 ml g^{-1}), as are values for K_d (1.5 ± 1.2 × 10^6 ml g^{-1}), for these
oceanic regions (Table 3). K_c values were estimated using the relationships $C_c/C_p = 2$
(Moran and Moore, 1989) and log $C_c = 0.7 \cdot$ log $C_p - 2.6$ (Honeyman and Santschi,
1989). With these values, K_c's range from 1.0 ± 1.1 × 10^5 ml g^{-1} using $C_c/C_p = 2$
(Moran and Moore, 1989) to 1.0 ± 1.2 × 10^6 ml g^{-1} using Honeyman and Santschi's
(1989) estimate for C_c.

4. Solid-solution partitioning of ^{234}Th as a function of particle concentration

Particle concentration, as a surrogate parameter for surface site concentration,
has been suggested (Honeyman *et al.,* 1988) as the master variable controlling the
scavenging of thorium and other reactive trace metals. The primary source of
particles onto which thorium is scavenged, particularly in the open ocean and
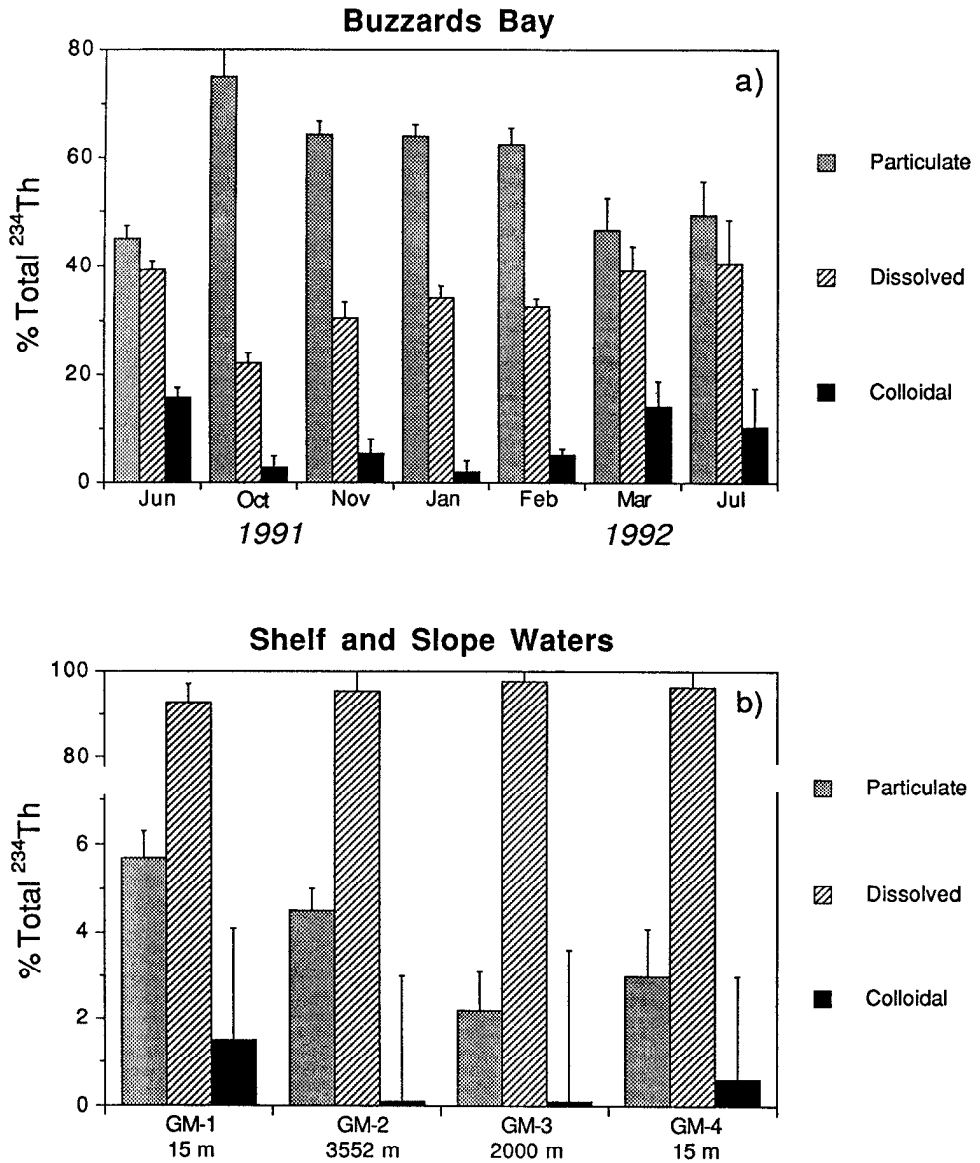upwelling regions, is biological production; indeed, scavenging rates of dissolved

Buzzards Bay

Shelf and Slope Waters

Figure 5. Partitioning of ^{234}Th between dissolved, colloidal, and particulate fractions in samples from (a) Buzzards Bay and (b) the shelf and slope waters from the Gulf of Maine cruise.

thorium correlate with new production (Bruland and Coale, 1986; Beals and Bruland, 1993). Moran and Moore (1989) and Honeyman and Santschi (1989) have further shown that the concentration of colloids is directly proportional to particle concentration. Thus, if particle concentration is the master variable controlling trace

Table 3. ^{234}Th partition coefficients.

Sample Code	K_d (10^5 ml g^{-1})	K_p (10^5 ml g^{-1})	K_c^* (10^5 ml g^{-1})	$K_c^\dagger$ (10^5 ml g^{-1})
BB-1	8.4	11.7	2.0	25.6
BB-2	16.8	18.8	0.3	5.2
BB-3	12.7	14.8	0.6	8.5
BB-4	14.1	14.9	0.2	3.0
BB-5	6.4	7.3	0.3	5.0
BB-6	18.2	24.8	3.8	38.0
BB-7	11.1	13.9	1.4	17.5
GM-1	6.0	6.1	0.8	5.1
GM-2	47.6	47.6	0.3	0.9
GM-3	22.6	22.6	0.4	1.2
GM-4	6.3	6.3	0.6	3.2

*Calculated using $C_c/C_p = 2$ (Moran and Moore, 1989).
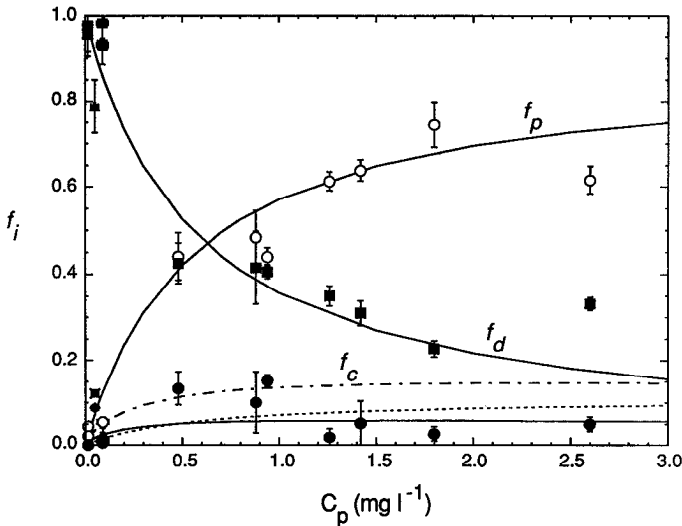†Calculated using $\log C_c = 0.7 \cdot \log C_p - 2.6$ (Honeyman and Santschi, 1989).

Figure 6. Partitioning of ^{234}Th between dissolved (■), colloidal (●), and particulate (○) phases as a function of suspended particle concentration (C_p) in samples from Buzzards Bay and the shelf and slope waters. Also shown are dissolved (▲), colloidal (◆), and particulate (×) ^{234}Th data for the upper ocean near Bermuda (Moran and Buesseler, 1992). Solid lines represent the fraction of dissolved (f_d) and particulate (f_p) ^{234}Th and were calculated (Appendix B) using the $K_p = 10^6$ ml g^{-1}. The fraction of colloidal ^{234}Th (f_c) is calculated using $K_p = 10^6$ ml g^{-1} and; (a) solid line, $\log C_c = 0.7 \cdot \log C_p - 2.6$ (Honeyman and Santschi, 1989) and $K_c = 10^6$ ml g^{-1} and; (b) dashed line, $C_c/C_p = 2$ (Moran and Moore, 1989) and $K_c = 10^5$ ml g^{-1}. Dash-dot line is an upper estimate of f_c calculated using $K_c = 2 \times 10^6$ ml g^{-1} and $\log C_c = 0.7 \cdot \log C_p - 2.6$.

metal scavenging, then the solid-solution partitioning of our size-fractionated [234]Th data would be expected to be a function of C_p.

The distribution of [234]Th between the various size classes shows a systematic dependence on suspended particle concentration (Fig. 6). The overall pattern of the solid-solution partitioning of [234]Th is a progressive shift from dissolved to particulate form with increasing C_p. The colloidal fraction follows the particulate distribution but to a lesser extent, increasing from the low C_p deep waters to the particle-rich shelf region. The colloidal [234]Th data shows some evidence of a maximum at $C_p =$ 0.5–1 mg l^{-1} and then decreases for $C_p > 1$ mg l^{-1}. Thus, in the surface open ocean and deep waters, where suspended particle concentrations and scavenging rates are lowest, [234]Th exists predominantly in the dissolved phase. With increasing C_p and hence scavenging rate in the surface shelf and slope waters, [234]Th is increasingly partitioned onto particulate and colloidal matter. In the particle-rich nearshore waters ($C_p \geq 1$ mg l^{-1}), where total activities are lowest due to intense scavenging and particle export, [234]Th is associated largely with particulate matter.

The dependence of the [234]Th size-distribution on C_p can be calculated using the partition coefficients K_p and K_c (Eqs. B1, B2; Appendix B). The fraction of dissolved (f_d) and particulate (f_p) [234]Th is calculated (Eqs. B6, B8) using our average $K_p =$ 10^6 ml g^{-1}. The fraction of colloidal [234]Th (f_c) is calculated (Eq. B7) using (a) $K_c =$ 10^5 ml g^{-1}, estimated using $C_c/C_p = 2$ (Moran and Moore, 1989) and (b) $K_c = 10^6$ ml g^{-1}, estimated from $\log C_c = 0.7 \cdot \log C_p - 2.6$ (Honeyman and Santschi, 1989). In addition, an upper estimate of f_c is calculated using $K_c = 2 \times 10^6$ ml g^{-1}.

The [234]Th size-distribution calculated using our measured partition coefficients is compared with the observed data in Figure 6. Good agreement exists between the observed and calculated distributions of dissolved and particulate [234]Th. For the colloidal fraction, both $K_c = 10^5$ ml g^{-1} (Moran and Moore, 1989) and $K_c = 10^6$ ml g^{-1} (Honeyman and Santschi, 1989) give essentially the same good agreement with the data for $C_p = 0.01$–1 mg l^{-1} and then diverge at $C_p \sim > 1$ mg l^{-1}. The higher colloidal values at $C_p \sim 0.5$–1 mg l^{-1} are more closely predicted using the upper estimate for K_c of 2×10^6 ml g^{-1}.

These results demonstrate the primary importance of the concentration of suspended particles and hence surface sites in controlling the size-distribution of [234]Th. In fact, the systematic dependence of [234]Th solid-solution partitioning on C_p suggests that C_p is a reasonable surrogate parameter for the surface functional groups that are likely to be involved in [234]Th sorption. This is particularly striking considering the potentially large range of particle types that were sampled within the different oceanic regimes.

5. [234]Th scavenging model

Estimates of the temporal and spatial variability in residence times of total and size-fractionated [234]Th are made using the box model shown in Figure 7. In this model, the activity of [234]Th is maintained by a balance between production from [238]U,
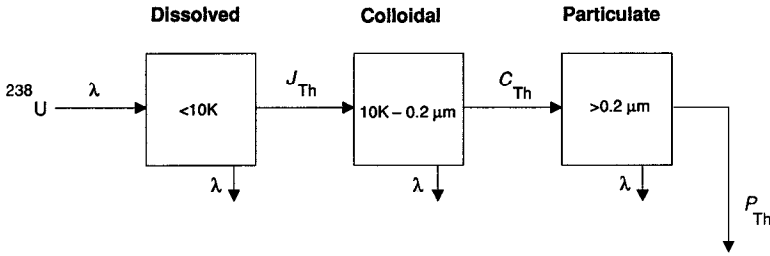
Figure 7. Scavenging model used to calculate residence times of ^{234}Th in the dissolved, colloidal, and particulate size classes (note: 10K represents 10,000 NMW). The terms J_{th}, C_{th} and P_{th} represent the net removal fluxes of ^{234}Th from the various size classes and λ is the ^{234}Th decay constant.

radioactive decay of ^{234}Th, and scavenging by colloidal and particulate matter. The model assumes irreversible scavenging of ^{234}Th and that advection and diffusion terms are negligible compared with net removal fluxes (Coale and Bruland, 1985, 1987; Buesseler *et al.*, 1992a; Moran and Buesseler, 1992). The differential equations for the surface water ^{234}Th scavenging model are:
for total ^{234}Th,

$$\partial A_{\text{Th}}^{\text{tot}}/\partial t = A_u \cdot \lambda - A_{\text{Th}}^{\text{tot}} \cdot \lambda - P_{\text{Th}} \tag{1}$$

and for ^{234}Th in each size class,

$$\partial A_{\text{Th}}^{d}/\partial t = A_u \cdot \lambda - A_{\text{Th}}^{d} \cdot \lambda - J_{\text{Th}} \tag{2}$$

$$\partial A_{\text{Th}}^{c}/\partial t = J_{Th} - A_{\text{Th}}^{c} \cdot \lambda - C_{\text{Th}} \tag{3}$$

$$\partial A_{\text{Th}}^{P}/\partial t = C_{Th} - A_{\text{Th}}^{P} \cdot \lambda - P_{\text{Th}} \tag{4}$$

where A_u is the ^{238}U activity, λ (0.0288 days^{-1}) is the decay constant of ^{234}Th, A^{tot} is the total ^{234}Th activity, A_{Th}^{d} is the dissolved ($<10{,}000$ NMW) activity, A_{Th}^{c} is the colloidal (10,000 NMW-0.2 μm) activity, and A_{Th}^{P} is the particulate (>0.2 μm) activity. The terms J_{Th}, C_{Th}, and P_{Th} represent the net removal flux of ^{234}Th from the dissolved to the colloidal phase, from colloids to particles, and of ^{234}Th on sinking particles, respectively (Fig. 7).

At steady-state ($\partial A_{\text{Th}}/\partial t = 0$), the mean residence time (τ) of ^{234}Th in the ith size-class is defined as (Moran and Buesseler, 1992),

$$\tau_i = A_{\text{Th}}^{i}/R_i \tag{5}$$

where A_{Th}^{i} is the ^{234}Th activity and R_i is the net removal flux. For the non-steady-state case ($\partial A_{\text{Th}}/\partial t \neq 0$), net removal fluxes are calculated assuming that the flux terms J_{Th}, C_{Th} and P_{Th} remain constant over a given time interval (Buesseler *et al.*, 1992a),

$$J_{\text{Th}} = \lambda \left[\frac{A_u(1 - e^{-\lambda t}) + A_{\text{Th}-1}^{d} e^{-\lambda t} - A_{\text{Th}-2}^{d}}{(1 - e^{-\lambda t})} \right] \tag{6}$$
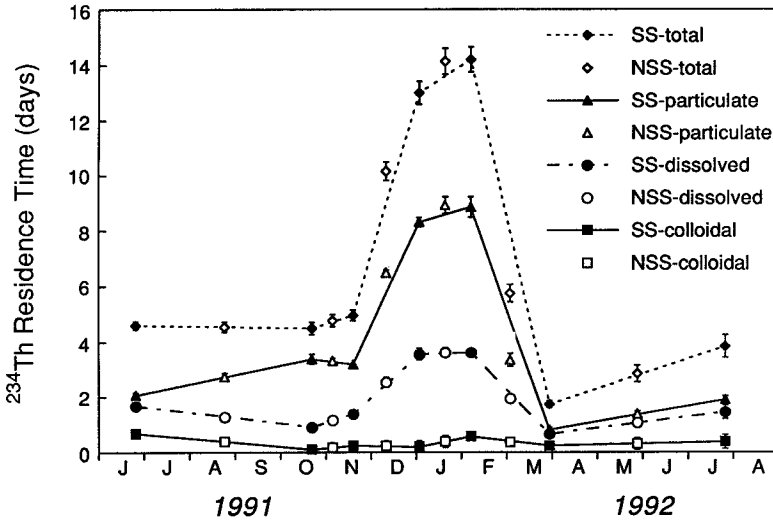
Figure 8. Temporal variability in residence times of dissolved, colloidal, particulate and total ^{234}Th in Buzzards Bay surface waters calculated for steady-state (SS) and non-steady-state (NSS) conditions.

$$C_{Th} = J_{Th} - \lambda \left[\frac{A^P_{Th-1}e^{-\lambda t} - A^P_{Th-2}}{(1 - e^{-\lambda t})} \right] \tag{7}$$

$$P_{Th} = \lambda \left[\frac{A_u(1 - e^{-\lambda t}) + A^{tot}_{Th-1}e^{-\lambda t} - A^{tot}_{Th-2}}{(1 - e^{-\lambda t})} \right] \tag{8}$$

where A_{Th-1} and A_{Th-2} are ^{234}Th activities at sampling times t_1 and t_2. For the non-steady-state case, the residence time of ^{234}Th in the ith size class is given by,

$$\tau_i = (A^i_{Th-2} + A^i_{Th-1})/2R_i \tag{9}$$

a. Temporal variability. In Buzzards Bay, temporal variations in the residence time of total and size-fractionated ^{234}Th are shown in Figure 8 and listed in Table 4. Residence times of total and size-fractionated ^{234}Th calculated for steady-state and non-steady-state conditions are short ($\sim$ <1–14 days), indicative of high scavenging rates occurring within the particle-rich nearshore waters. Throughout the annual cycle, colloidal ^{234}Th residence times are low, averaging 0.3 days, and show only a slight seasonal variation. By comparison, residence times of dissolved and particulate ^{234}Th are higher, averaging 2 days and 4 days, respectively. In addition, unlike the colloidal fraction, the dissolved and particulate ^{234}Th residence times exhibit a strong seasonal cycle, with maximum values observed during the winter.

The steady-state and non-steady-state models provide comparable ^{234}Th residence times, with the steady-state results bracketing the non-steady-state values over each

Table 4. Residence times (in days) of dissolved (τ_d) colloidal (τ_c), particulate (τ_p) and total (τ_{tot}) ^{234}Th calculated using the irreversible scavenging model (Fig. 7) for steady-state and non-steady-state (shown in parentheses) conditions.*

Sample Code	τ_d	τ_c	τ_p	τ_{tot}
BB-1	1.68 ± 0.05	0.68 ± 0.08	2.08 ± 0.09	4.62 ± 0.13
	(1.28 ± 0.07)	(0.38 ± 0.07)	(2.74 ± 0.14)	(4.56 ± 0.18)
BB-2	0.91 ± 0.06	0.11 ± 0.09	3.39 ± 0.18	4.51 ± 0.22
	(1.16 ± 0.10)	(0.18 ± 0.10)	(3.33 ± 0.10)	(4.79 ± 0.22)
BB-3	1.38 ± 0.12	0.24 ± 0.12	3.2 ± 0.02	4.98 ± 0.19
	(2.55 ± 0.18)	(0.23 ± 0.18)	(6.5 ± 0.10)	(10.16 ± 0.33)
BB-4	3.57 ± 0.21	0.20 ± 0.21	8.32 ± 0.17	13.01 ± 0.42
	(3.63 ± 0.17)	(0.38 ± 0.21)	(8.93 ± 0.30)	(14.15 ± 0.47)
BB-5	3.63 ± 0.11	0.57 ± 0.13	8.86 ± 0.37	14.21 ± 0.13
	(1.96 ± 0.10)	(0.37 ± 0.15)	(3.36 ± 0.24)	(5.76 ± 0.31)
BB-6	0.66 ± 0.06	0.24 ± 0.08	0.86 ± 0.08	1.74 ± 0.13
	(1.07 ± 0.17)	(0.31 ± 0.20)	(1.38 ± 0.11)	(2.86 ± 0.30)
BB-7	1.46 ± 0.25	0.38 ± 0.26	1.91 ± 0.14	3.86 ± 0.41
GM-1	29.17 ± 1.08	0.47 ± 0.84	1.91 ± 0.19	33.60 ± 1.76
GM-2	102.43 ± 9.84	0.06 ± 3.17	5.69 ± 1.06	125.14 ± 19.61
GM-3	127.59 ± 17.48	0.09 ± 4.61	3.15 ± 1.46	142.78 ± 30.55
GM-4	85.75 ± 4.29	0.54 ± 2.18	2.98 ± 1.13	98.11 ± 9.44

*Errors propagated from counting statistics.

sampling interval (Fig. 8; Table 4). This agreement can be attributed to the extent of ^{234}Th/^{238}U disequilibria being large throughout the year and to the relatively small changes in $\partial A_{Th}^{tot}/\partial t$ (Fig. 3). Wei and Murray (1992) also reported good agreement for ^{234}Th residence times calculated using steady-state and non-steady-state models during monthly sampling in Dabob Bay, WA. A non-steady-state model is required when significant changes in ^{234}Th activity occur over short time-scales (e.g. 1–2 weeks), for example during phytoplankton blooms (Tanaka *et al.,* 1983; Buesseler *et al.,* 1992a).

The seasonal cycle in the residence time of total ^{234}Th is presumably a function of temporal changes in biological production and sediment resuspension rates. The shorter residence times of ^{234}Th observed during the summer may result from elevated rates of biological production that lead to enhanced scavenging of ^{234}Th from the water column. Figure 3 shows that C_p values were not particularly high during the summer, however we may have missed short-term increases in C_p. During the winter, when biological activity is typically reduced in these waters (Glibert *et al.,* 1982, 1985), ^{234}Th residence times are greater. The main exception to this is during the winter bloom, when biological processes evidently played an important role in the removal of total ^{234}Th (Fig. 3).

In addition, studies of particle concentration and flux (measured by sediment traps) in Long Island Sound showed that an important factor in the settling flux of
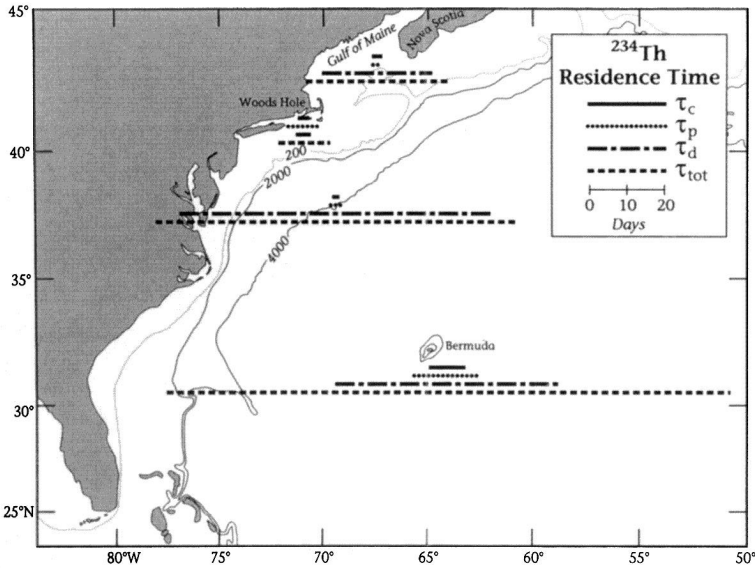
Figure 9. Spatial variability in residence times of total (τ_{tot}) and size-fractionated ^{234}Th (τ_c, colloidal; τ_p, particulate; τ_d, dissolved) in the surface waters. Residence times are calculated for steady-state conditions and are proportional to the length of the line shown in the legend. Data near Bermuda from Moran and Buesseler (1992).

^{234}Th was the viscosity of seawater (J. K. Cochran, personal communication), which is temperature-dependent and thus at a maximum in the winter. High viscosity can result in lower settling velocities of particles and hence a lower ^{234}Th sedimentation flux. Santschi *et al.* (1979) reported a similar seasonal cycle in ^{234}Th residence times in Narragansett Bay and suggested the residence time of ^{234}Th was longer in the winter due, in part, to a higher water viscosity.

The higher ^{234}Th activities and corresponding longer residence times during the winter may also be attributed to an input of ^{234}Th from resuspended bottom sediments. Martin and Sayles (1987) reported an average total of ^{234}Th sediment activity (supported plus excess) of 5.5 ± 1.9 dpm g^{-1} over an annual cycle in the upper 2–3 cm (depth of bioturbation) in Buzzards Bay. Our measured specific activity of particulate ^{234}Th in the water column is $\sim$100–300 dpm g^{-1}. Using our highest particle concentration of 2.6 mg l^{-1} and the average sediment ^{234}Th activity, the contribution of ^{234}Th from resuspended sediments is estimated to be 0.014 dpm l^{-1}, or <5% of total ^{234}Th in the water column. This estimate is a lower limit since resuspended material may have a higher ^{234}Th activity than the average activity of the upper 2–3 cm of sediment.

b. Spatial variability. The spatial variability in residence times of total and size-fractionated ^{234}Th in the surface waters is shown in Figure 9. As expected from the

total activities (Fig. 1), total ^{234}Th residence times increase from the nearshore to the surface open ocean, consistent with enhanced scavenging and export of ^{234}Th from the water column occurring within the particle-rich shelf waters. The residence time of colloidal ^{234}Th does not exhibit significant spatial variability, increasing only slightly in the Gulf of Maine (~ 0.4 days) and beyond the shelf break (~ 0.5 days), with the highest value (10 days) found near Bermuda (cf, Moran and Buesseler, 1992). In addition, colloidal ^{234}Th residence times are consistently short compared with values determined for the dissolved phase of 1–4 days in Buzzards Bay, ~ 30 days in the Gulf of Maine and 61–85 days in the surface open ocean. By comparison, particulate ^{234}Th residence times are within a factor of about 2–3 of the colloidal fraction in the Gulf of Maine and the surface open ocean.

It is evident that the residence time of colloidal ^{234}Th is consistently short and does not exhibit the degree of temporal or spatial variability as observed for dissolved ^{234}Th. The relative constancy of the colloidal ^{234}Th residence time would seem surprising, given the range in total activity and hence overall scavenging intensity. For example, the dissolved ^{234}Th residence time varies by a factor of ~ 30–40 between the nearshore and the surface open ocean. By comparison, colloidal ^{234}Th residence times vary by a factor of ~ 2–10, similar to the ~ 4–5 fold variation for the particulate fraction. The short and relatively constant colloidal ^{234}Th residence times may be at least partly related to our model which does not include terms for disaggregation and therefore provides minimum estimates of ^{234}Th residence times. However, as discussed later, these results would imply that colloidal aggregation is not a rate-limiting step in thorium scavenging. In fact, colloidal ^{234}Th may be tracing a reactive intermediate in the decomposition of large, rapidly-sinking biogenic particles.

6. Particle-concentration effects

Evidence for the involvement of colloids in oceanic trace metal scavenging comes primarily from observations of: (1) distribution coefficients (K_d's) for thorium and other particle-reactive species that vary inversely with C_p and; (2) a less than 1:1 log-log correlation between scavenging rate constants (k'_1) for thorium and C_p (e.g. Gschwend and Wu, 1985; Morel and Gschwend, 1987; Honeyman *et al.*, 1988; Moran and Moore, 1989). These so-called "particle-concentration effects" have been interpreted as resulting from the inclusion of colloids in an operationally defined "dissolved" (< 0.2 μm) phase. The size-fractionated ^{234}Th data can be used to examine under what oceanic regimes such particle-concentration effects are manifest.

Figure 10 shows a log-log plot of K_d values for ^{234}Th against C_p. The K_d values are calculated (Eq. B3, Appendix B) using the size-fractionated ^{234}Th data reported in this study and from the upper ocean near Bermuda (Moran and Buessler, 1992). Also plotted are K_p values for the partitioning of ^{234}Th between dissolved ($< 10,000$
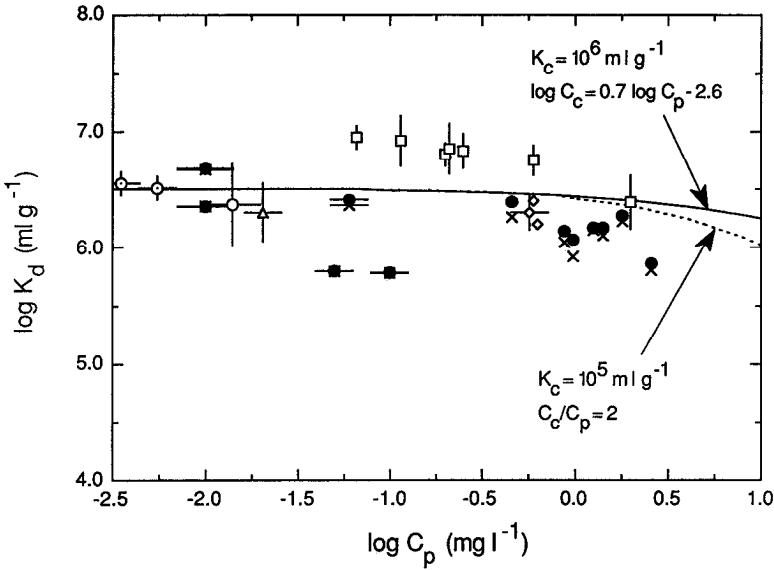
Journal of Marine Research

Figure 10. Log-log plot of ^{234}Th K_d values against suspended particle concentration (C_p) calculated using ($\times$) the size-fractionated ^{234}Th data reported in this study and from the upper ocean near Bermuda (Moran and Buesseler, 1992); also shown are ($\bullet$) K_p values for the partitioning of ^{234}Th between dissolved ($< 10,000$ NMW) and particulate ($> 0.2 \ \mu$m) phases. Data defined by open symbols (after Honeyman *et al.*, 1988 and Moran and Moore, 1992): $\odot$, surface and deep Arctic Ocean (Bacon *et al.*, 1989); $\triangle$, deep western Pacific (Nozaki *et al.*, 1987); $\bigcirc$, deep eastern Pacific (Bacon and Anderson, 1982); $\square$, California Current (Coale and Bruland, 1985), $\diamond$, Funka Bay, Japan (Minagawa and Tsunogai, 1980). Lines calculated (Appendix B) using $K_p = 10^{6.5}$ ml g^{-1} and: 1) solid line, $K_c = 10^6$ ml g^{-1} and $\log C_c = 0.7 \cdot \log C_p - 2.6$ (Honeyman and Santschi, 1989); 2) dashed line, $K_c = 10^5$ ml g^{-1} and $C_c/C_p = 2$ (Moran and Moore, 1989).

NMW) and particulate ($> 0.2 \ \mu$m) phases. For comparison, K_d values are included from independent studies in which the "dissolved" and particulate phase was defined using 0.2–0.4 μm filters and the colloidal fraction was not reported. As shown in Figure 10, K_d values are slightly lower than the respective K_p values for $C_p \sim 1$ mg l^{-1}, where colloidal ^{234}Th activities are highest. Importantly, within the scatter of the data, K_d values are essentially invariant over the C_p range characteristic of oceanic waters (~ 0.01–1 mg l^{-1}).

The relationship between K_d and C_p can be quantified using (Appendix B),

$$K_d = \frac{K_p}{1 + K_c \cdot C_c}. \tag{10}$$

Eq. 10 was used to calculate the dependence of K_d on C_p using a constant $K_p = 10^{6.5}$ ml g^{-1} and our estimated values of K_c and C_c: (1) $K_c = 10^6$ ml g^{-1} and $\log C_c = 0.7 \cdot \log C_p - 2.6$ (Honeyman and Santschi, 1989) and; (2) $K_c = 10^5$ ml g^{-1} and $C_c/C_p = 2$
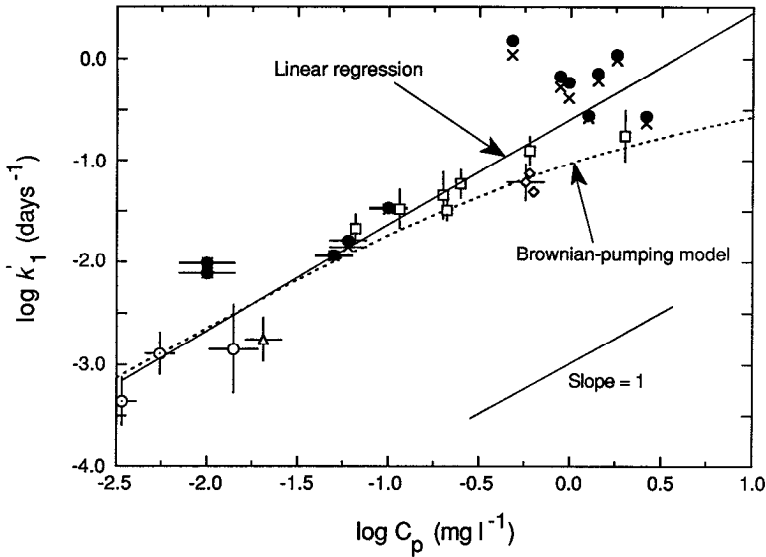
Figure 11. Log-log plot of forward scavenging rate constants (k'_1) for ^{234}Th against suspended particle concentration (C_p) calculated using (●) dissolved ($<10,000$ NMW) ^{234}Th and (×) dissolved ($<10,000$ NMW) + colloidal (10,000 NMW-0.2 μm) ^{234}Th data reported here and for the upper ocean near Bermuda (Moran and Buesseler, 1992). Open symbols are defined in Figure 10. Solid line is linear regression of all data. Dashed line represents an upper limit for scavenging rate constants predicted by the Brownian-pumping model calculated using $k'_1 = B_b \cdot C_p^{0.3} \cdot f_{c/d}$ (Eq. 11). Critical coagulation parameters are $h = 6$ m, $\alpha_b = 0.5$, $\rho_e = 2.5$ g cm^{-3}, $K_c = 10^7$ ml g^{-1} and $\log C_c = 0.7 \cdot \log C_p - 2.6$ (Honeyman and Santschi, 1989).

(Moran and Moore, 1989). Figure 10 shows the calculated K_d is constant for $C_p \sim$ 0.01–1 mg l^{-1}, consistent with the data, and then decreases for $C_p > 1$ mg l^{-1}.

It is evident from our size-fractionated ^{234}Th data and model calculations that particle-concentration effects on K_d are essentially negligible for most oceanic waters. That is, there is no strong evidence for an inverse relation between K_d and C_p (Fig. 10).

Figure 11 shows a log-log plot of k'_1 values for ^{234}Th against C_p. Net scavenging rate constants for the removal of dissolved ($<10,000$ NMW) ^{234}Th onto colloidal matter are defined as $k'_1 = 1/\tau_d$ and are calculated using the size-fractionated data reported here and from the surface waters near Bermuda (Moran and Buesseler, 1992). Values of k'_1 were also calculated for the net removal of "dissolved" ^{234}Th ($A^d_{Th} + A^c_{Th}$) onto particulate matter. For comparison, scavenging rate constants are plotted using data from independent studies in which the colloidal fraction was not sampled. Scavenging rate constants calculated using the "dissolved" activities are slightly lower than the respective dissolved values in Buzzards Bay, where colloidal activities represent a higher percentage of the total (Fig. 11). However, within the scatter of

the data, it is clear that $\partial \log k'_1 / \partial \log C_p \sim 1$, indicating a first-order dependence of k'_1 on C_p.

Figure 11 also shows scavenging rate constants for thorium calculated using the Brownian-pumping model (Honeyman and Santschi, 1989) as a function of C_p. In this model, the rate of transfer of metals from dissolved to particulate form is limited by the rate of colloid-particle aggregation. Scavenging rate constants were calculated as a function of C_p using the Brownian coagulation coefficient (B_b) and the fraction ($f_{c/d}$) of "dissolved" (<0.2 μm) ^{234}Th associated with colloids,

$$k'_1 = B_b \cdot C_p^{0.3} \cdot f_{c/d} \tag{11}$$

B_b was calculated using values suggested by Honeyman and Santschi (1989) for the critical coagulation parameters of $h = 6$ m, $\alpha_b = 0.5$ and $\rho_e = 2.5$ g cm^{-3} (Appendix C). As noted by Moran and Moore (1992), because ρ_e and α_b are upper estimates and h is a lower estimate, the calculated rate constants represent maximum values. Figure 11 shows the predicted scavenging rate constants diverge from the linear regression line with increasing C_p. However, the predicted values are consistent with the data for $C_p \sim 0.01$–1 mg l^{-1}.

The relatively high rate constants for Buzzards Bay ($C_p \sim 1$ mg l^{-1}) compared with the model curve (Fig. 11) may be due to higher shear coagulation caused by high energy dissipation rates from tidal mixing. Honeyman and Santschi (1992) reported a good agreement between ^{234}Th scavenging rate constants determined for the Irish Sea and predicted rate constants that included a term for shear coagualtion. These authors assumed an energy dissipation rate of 2.3×10^{-3} m^2 s^{-3} in the bottom boundary layer, a value which is relatively high compared with dissipation rates of $2 \times 10^{-7} - 6 \times 10^{-4}$ m^2 s^{-3} reported for coastal waters. Assuming a similar energy dissipation rate in the bottom boundary layer in Buzzards Bay, the predicted rate constant at $C_p = 1$ mg l^{-1} is $\sim 10^{-0.5}$ day^{-1}, which is consistent with ^{234}Th scavenging rate constants determined for Buzzards Bay (Fig. 11).

It is important to note that the mechanisms controlling the apparent first-order dependence of k'_1 on C_p (Fig. 11) are not well characterized. This is likely to include a combination of surface-adsorption and Brownian and shear coagulation/sedimentation processes. Based on our size-fractionated ^{234}Th data, there is no evidence for particle-concentration effects causing a less than unity dependence of k'_1 on C_p (Fig. 11) that would be expected from rate-limiting aggregation of colloids controlling the removal of thorium. Moran and Moore (1992) made a similar observation in a comparative study of oceanic scavenging rate constants of aluminum and thorium.

7. Summary and implications for the role of colloids in oceanic trace metal scavenging

The size-fractionated ^{234}Th results presented here indicate that 1–16% of total ^{234}Th is in the high molecular weight colloidal size range. The activity of colloidal

^{234}Th is a function of the suspended particle concentration, with higher colloidal values observed in the particle-rich nearshore region. Our results are generally consistent with the few recent oceanographic studies of colloidal ^{234}Th. In particular, Moran and Moore (1989) conducted ^{234}Th tracer experiments using colloids (10,000 NMW-0.45 μm) collected off Nova Scotia and reported colloidal ^{234}Th activities of 1–4% of "dissolved" (<0.45 μm) in shelf and slope waters and, in one sample, up to 50% in nearshore waters. In the upper ocean near Bermuda, Moran and Buesseler (1992) reported colloidal ^{234}Th activities averaging 9% of the total activity. Niven (personal communication) recently measured colloidal ^{234}Th (10,000 NMW-0.2 μm) during a phytoplankton bloom in Bedford Basin and found activities ranging from 1–15% of the total activity. The highest oceanic colloidal ^{234}Th activities have been reported for the Gulf of Mexico (Baskaran *et al.*, 1992), where colloidal ^{234}Th (10,000 NMW-0.4 μm) averaged 28 ± 14% of the total activity in 6 of 14 samples for which total activities could be calculated.

The importance of these results is that what is considered as "dissolved" can in fact exist to a significant extent in a colloidal form, particularly in nearshore waters. Our results indicate that up to ~30% of traditionally defined "dissolved" (<0.2 μm) ^{234}Th is in the high molecular weight colloidal size range in Buzzards Bay. The implication is that scavenging of thorium, and by analogy other particle-reactive trace metals, may involve coagulation-disaggregation processes rather than adsorption-desorption reactions on particle surfaces alone.

It is surprising that coefficients for the partitioning of ^{234}Th between dissolved and colloidal forms (K_c) are less than, or in some cases similar to, K_p values determined for dissolved and particulate forms. Baskaran *et al.* (1992) also reported similar K_p and K_c values for ^{234}Th in the Gulf of Mexico. As discussed by Moore and Hunter (1985), based on particle surface area, one would expect colloids to have a greater capacity than larger particles (>0.2 μm) for adsorbing trace metals and hence $K_c \gg K_p$. However, our results indicate that the thorium complexation capacity and hence binding site density of colloidal and particulate matter is similar. This would imply that the thorium binding site density of marine particles may not increase markedly in the submicron size range, despite the increase in surface area per unit mass. It is important to note, however, that the concentration and nature of binding sites of marine colloidal matter is not well characterized.

Based on the irreversible scavenging model, residence times of colloidal ^{234}Th are short, ranging from <1 day in the shelf waters to ~10 days in the upper ocean near Bermuda. Moreover, while dissolved and particulate ^{234}Th residence times exhibit significant temporal and spatial variability, this is not observed for colloidal ^{234}Th. The short and relatively invariant residence time of colloidal ^{234}Th would imply that colloidal aggregation is not a rate-limiting step in thorium scavenging, which clearly does vary spatially with particle concentration and flux (Figs. 1, 9). Such rapid turnover rates are evidently not representative of the bulk of "dissolved" organic

matter, which has a mean ^{14}C age on the order of ~ 1000 years in the surface waters of the Atlantic and Pacific (Bauer *et al.*, 1992).

Our short colloidal ^{234}Th residence times would imply that ^{234}Th is tracing some component of colloidal organic matter that is labile and rapidly turning over in the upper ocean, possibly involving heterotrophic activity (Kirchman *et al.*, 1991; Benner *et al.*, 1992). This is consistent with the view of particle cycling linked to bacterial decomposition and hydrolytic enzyme activity proposed by Cho and Azam (1988), Karl *et al.* (1988) and more recently by Smith *et al.* (1992). These studies provide evidence for the importance of large-scale production of suspended particles via bacterially mediated decomposition of large biogenic aggregates. It is possible that a major fraction of organic-rich colloids are also generated by heterotrophic decomposition of large biogenic particles. An important implication of our observations is that the dominant pathway in our particle cycling model (Fig. 7) may be in the reverse direction; large biogenic particles → organic-rich colloids → dissolved organic matter. Thorium may be released from fast-sinking particles as they decompose, or retained preferentially relative to organic carbon, but in either case the result may be a K_c which is smaller than K_p. Thus, colloidal ^{234}Th may be tracing a reactive intermediate in the decomposition of large, rapidly-sinking biogenic particles into colloids and DOM.

The size-fractionated ^{234}Th results indicate that so-called "particle-concentration effects" are negligible for most oceanic waters ($C_p \sim 0.01$–1 mg l^{-1}). Furthermore, because ^{234}Th is highly particle-reactive ($K_d \sim 10^6$–10^7 ml g^{-1}), the association of ^{234}Th with colloids and hence the corresponding particle-concentration effect is likely to be greater for thorium than for less reactive trace metals. For example, Moran and Moore (1989, 1992) demonstrated that aluminum ($K_d \sim 10^6$ ml g^{-1}) is associated to a lesser extent with colloids and that particle-concentration effects are reduced compared with thorium. In terms of using K_d's to model trace metal transport in aqueous systems, our data suggest that an inverse dependence of K_d on C_p may be significant in regions characterized by high particle concentrations ($C_p > \sim 1$ mg l^{-1}), such as freshwaters, estuaries, nearshore waters, pore-waters and groundwater environments.

It is important to consider the possible significance of colloidal matter in the 1,000–10,000 NMW size range. In this regard, Benner *et al.* (1992) reported 22–33% of "dissolved" (<0.2 μm) organic carbon was in the 1,000 NMW-0.2 μm colloidal size range off Hawaii. These data are consistent with results of Carlson *et al.* (1985), who reported $\sim 34\%$ of persulphate-oxidizable "dissolved" organic carbon was $>1,000$ NMW in North Atlantic surface waters. By comparison, Moran and Moore (1989) found organic carbon concentrations in the 10,000 NMW-0.45 μm colloidal size range represented 5–15% of UV-photooxidizable organic carbon (<0.45 μm) in the shelf and slope waters off Nova Scotia. It is interesting that this range (5–34%)

for the percentage of "dissolved" organic carbon in the high molecular weight size range is consistent with estimates by Wells and Goldberg (1991) that the recently observed submicron particles (Koike *et al.,* 1990; Wells and Goldberg, 1991; Long-hurst *et al.,* 1992) may account for $\sim 10\%$ of DOC. These results suggest that there is a pool of organic carbon in the 1,000–10,000 NMW size range that would not be sampled using our 10,000 NMW filter. However, these data also suggest that (assuming a constant Th/C ratio) inclusion of a 1,000–10,000 NMW fraction would increase our colloidal ^{234}Th activities from ~ 5–15% to ~ 20–30% of the total for $C_p \sim 0.05$–0.1 mg l^{-1} (Fig. 6). Moreover, such a higher fraction (f_c) of ^{234}Th associated with colloids can be reasonably predicted from (Appendix B),

$$f_c = \frac{A_{Th}^c}{A_{Th}^{tot}} = \frac{K_c \cdot C_c}{\Sigma} \tag{12}$$

and using $K_c = 10^7$ ml g^{-1} and log $C_c = 0.7 \cdot$ log $C_p - 2.6$ (Honeyman and Santschi, 1989), although this needs to be confirmed.

It is important to emphasize that our understanding of the mechanisms of oceanic trace metal scavenging and particle cycling is limited. The irreversible box model (Fig. 7) provides useful information on the residence times and scavenging rate constants for ^{234}Th. However, as noted above, it is apparent that reverse processes, i.e. desorption, disaggregation, and bacterial remineralization, are important in trace metal scavenging and particle cycling in the water column (Bacon and Anderson, 1982; Nozaki *et al.,* 1981, 1987; Clegg and Whitfield, 1990, 1991; Cho and Azam, 1988; Karl *et al.,* 1988; Smith *et al.,* 1992). A key area for future research is to quantify the complex interplay between the chemical, biological, and physical processes that control metal-particle and particle-particle interactions throughout the size spectrum. One approach to this problem is to measure at least two thorium isotopes, as this would allow the mechanisms of scavenging and particle cycling to be investigated using a reversible model (e.g. Murnane *et al.,* 1990; Clegg and Whitfield, 1990, 1991; Cochran *et al.,* 1993).

APPENDIX A

Symbols

α_b = Brownian collision efficiency factor

A_{Th} = ^{234}Th activity (dpm l^{-1})

A_u = ^{238}U activity (dpm l^{-1})

B_b = Brownian coagulation coefficient (l$^{0.3}$ mg$^{-0.3}$ day^{-1})

C_c = colloid concentration (mg l^{-1})

C_p = suspended particle concentration (mg l^{-1})

f_c = fraction of total ^{234}Th associated with colloids (10,000 NMW-0.2 μm)

f_d = fraction of total ^{234}Th in dissolved (< 10,000 NMW) form

$f_{c/d}$ = fraction of "dissolved" (< 0.2 μm) ^{234}Th associated with colloids

f_p = fraction of total ^{234}Th in particulate (> 0.2 μm) form

g = gravitational acceleration (980 cm s^{-2})

h = mixed depth (m)

k = Boltzman constant (erg °K^{-1})

k_1' = pseudo-first-order scavenging rate constant for dissolved ^{234}Th (days^{-1})

K_b = Brownian coagulation kernel (cm^3 s^{-1})

K_c = partition coefficient for ^{234}Th in colloidal and dissolved forms (ml g^{-1})

K_d = partition coefficient for ^{234}Th in particulate and "dissolved" forms (ml g^{-1})

K_p = partition coefficient for ^{234}Th in particulate and dissolved forms (ml g^{-1})

λ = ^{234}Th decay constant (days^{-1})

ρ_e = particle density (g cm^{-3})

ρ_f = fluid density (g cm^{-3})

R_i = net removal flux of ^{234}Th (dpm l^{-1} days^{-1})

S/h = dimensional parameter grouping for Stokes settling (cm^{-2} s^{-1})

Σ = A_{Th}^{tot}/A_{Th}^d

T = absolute temperature (°K)

τ = residence time (days)

μ = dynamic viscosity (g cm^{-1} s^{-1})

ν = kinematic viscosity (cm^2 s^{-1})

APPENDIX B

Partitioning of ^{234}Th between dissolved, colloidal and particulate forms

Coefficients for the partitioning of ^{234}Th between the dissolved and particulate phase (K_p), the dissolved and colloidal phase (K_c), and between the traditionally defined "dissolved" (< 0.2 μm) and particulate phase (K_d) are given by (Honeyman and Santschi, 1989; Moran and Moore, 1989) (units: ml g^{-1}),

$$K_p = \frac{A_{Th}^p}{A_{Th}^d} \cdot \frac{10^6}{C_p} \tag{B1}$$

$$K_c = \frac{A^c_{Th}}{A^d_{Th}} \cdot \frac{10^6}{C_c} \tag{B2}$$

$$K_d = \frac{A^p_{Th}}{(A^d_{Th} + A^c_{Th})C_p} = \frac{K_p}{1 + K_c \cdot C_c}. \tag{B3}$$

As shown by Honeyman and Santschi (1989), since

$$A^{tot}_{Th} = A^d_{Th} + A^c_{Th} + A^p_{Th} \tag{B4}$$

then

$$A^{tot}_{Th} = A^d_{Th}\{(K_c \cdot C_c) + (K_p \cdot C_p) + 1\} = A^d_{Th} \cdot \Sigma. \tag{B5}$$

From Eqs. (B1–B5), the fraction of ^{234}Th in the dissolved (f_d), colloidal (f_c), and particulate (f_p) size class is defined as,

$$f_d = \frac{A^d_{Th}}{A^{tot}_{Th}} = \frac{1}{\Sigma} \tag{B6}$$

$$f_c = \frac{A^c_{Th}}{A^{tot}_{Th}} = \frac{K_c \cdot C_c}{\Sigma} \tag{B7}$$

$$f_p = \frac{A^p_{Th}}{A^{tot}_{Th}} = \frac{K_p \cdot C_p}{\Sigma} \tag{B8}$$

APPENDIX C

Scavenging rate constants calculated using the Brownian-pumping model

In the Brownian-pumping, or colloidal-pumping, model (Honeyman and Santschi, 1989, 1992), the Brownian coagulation coefficient (B_b) is calculated from (Farley and Morel, 1986)

$$B_b = 1.33 \, (S/h)^{0.6} \rho_e^{-0.3} \alpha_b^{0.4} K_b^{0.4} \tag{C1}$$

$$S/h = (1/6\pi^2)^{0.33}(g/3vh)(\rho_e - \rho_f)/\rho_f \tag{C2}$$

$$K_b = 2kT/3\mu. \tag{C3}$$

Oceanic values for the various parameters suggested by Honeyman and Santschi (1989) are: $h = 6$ m; $\rho_e = 2.5$ g cm^{-3}; $\alpha_b = 0.5$ (Edzwald *et al.*, 1974); $g = 980$ cm s^{-2}; $v = 0.0098$ cm^2 s^{-1}; $\rho_f = 1.025$ g cm^{-3}; $\mu = 0.01$ g cm^{-1} s^{-1}; $k = 1.4 \times 10^{-16}$ erg °K^{-1}; and, $T = 293$°K. While some of the terms in Eqs. (C1, C2, C3) are clearly not constant for oceanic waters, B_b is affected most significantly by h, ρ_e, and α_b (Honeyman and Santschi, 1989; Moran and Moore, 1992). With these values, the Brownian coagulation coefficient is $B_b = 1.47 \times 10^{-1}$ l$^{0.3}$ mg$^{-0.3}$ day^{-1}. As discussed earlier, shear coagulation becomes significant in high-energy coastal waters, and estimates are

made of scavenging rate constants that include shear coagulation in Buzzards Bay (Section 6). The fraction of "dissolved" (<0.2 μm) metal associated with colloids ($f_{c/d}$) is given by,

$$f_{c/d} = \frac{f_c}{f_c + f_d} = \frac{K_c \cdot C_c}{(1 + K_c \cdot C_c)} \tag{C4}$$

When $f_{c/d} = 1$, all "dissolved" metal is associated with colloids and removed at a maximum rate; the rate of particle coagulation by Brownian motion. Values of $f_{c/d}$ are calculated using $K_c = 10^7$ ml g^{-1} and log $C_c = 0.7 \cdot$ log $C_p - 2.6$ (Honeyman and Santschi, 1989).

REFERENCES

Anderson, R. F. and A. P. Fleer. 1982. Determination of natural actinides and plutonium in marine particulate material. Anal. Chem., *54*, 1142–1147.

Bacon, M. P. and R. F. Anderson. 1982. Distribution of thorium isotopes between dissolved and particulate forms in the deep sea. J. Geophys. Res., *87*, 2045–2056.

Bacon, M. P., C.-H Huh and R. M. Moore. 1989. Vertical profiles of some natural radionuclides over the Alpha Ridge, Arctic Ocean. Earth Planet. Sci. Lett., *95*, 15–22.

Baskaran, M., P. H. Santschi, G. Benoit and B. D. Honeyman. 1992. Scavenging of thorium isotopes by colloids in seawater of the Gulf of Mexico. Geochim. Cosmochim. Acta, *56*, 3375–3388.

Bauer, J. E., P. M. Williams and E. R. M. Druffel. 1992. [14]C activity of dissolved organic carbon fractions in the north-central Pacific and Sargasso Sea. Nature, *357*, 667–670.

Beals, D. M. and K. W. Bruland. 1993. Scavenging of [234]Th in the Pacific Ocean. Deep-Sea Res., (in press).

Benner, R., J. D. Pakulski, M. McCarthy, J. I. Hedges and P. G. Hatcher. 1992. Bulk chemical characteristics of dissolved organic matter in the ocean. Science, *255*, 1561–1564.

Bruland, K. W. and K. H. Coale. 1986. Surface water [234]Th:[238]U disequilibria: spatial and temporal variations of scavenging rates within the Pacific Ocean, *in* Dynamic Processes in the Chemistry of the Upper Ocean, J. D. Burton, P. G. Brewer and R. Chesselet, eds., NATO Conference Series IV, Plenum Press, 159–172.

Buesseler, K. O., M. P. Bacon, J. K. Cochran and H. D. Livingston. 1992a. Carbon and nitrogen export during the JGOFS North Atlantic Bloom Experiment estimated from [234]Th:[238]U disequilibria. Deep-Sea Res., *39*, 1115–1137.

Buesseler, K. O., M. P. Bacon, J. K. Cochran, H. D. Livingston, S. A. Casso, D. Hirschberg, M. C. Hartman and A. P. Fleer. 1992b. Determination of thorium isotopes in seawater by non-destructive and radiochemical procedures. Deep-Sea Res., *39*, 1103–1114.

Carlson, D. J., M. L. Brann, T. H. Hague and L. M. Mayer. 1985. Molecular weight distribution of dissolved organic materials in seawater determined by ultrafiltration. Mar. Chem., *16*, 155–171.

Chen, J. H., R. L. Edwards and G. J. Wasserburg. 1986. [238]U, [234]U, and [232]Th in seawater. Earth Planet. Sci. Lett., *80*, 241–251.

Cho, B. C. and F. Azam. 1988. Major role of bacteria in biogeochemical fluxes in the ocean's interior. Nature, *332*, 441–443.

Clegg, S. L. and M. Whitfield. 1990. A generalized model for the scavenging of trace metals in the open ocean—I. Particle cycling. Deep-Sea Res., *37*, 809–832.

—— 1991. A generalized model for the scavenging of trace metals in the open ocean—II. Thorium scavenging. Deep-Sea Res., *38,* 91–120.

Coale, K. H. and K. W. Bruland. 1985. ^{234}Th:^{238}U disequilibria within the California Current. Limnol. Oceanogr., *30,* 22–33.

—— 1987. Oceanic stratified euphotic zone as elucidated by ^{234}Th:^{238}U disequilibria. Limnol. Oceanogr., *32,* 189–200.

Cochran, J. K., M. P. Bacon, K. O. Buesseler and H. D. Livingston. 1993. Thorium isotopes as indicators of particle dynamics in the upper ocean: results from the North Atlantic Bloom Experiment. Deep-Sea Res. *40,* 1569–1595.

Edzwald, J. K., J. C. Upchurch and C. R. O'Melia. 1974. Coagulation in estuaries. Environ. Sci. Tech., *8,* 58–63.

Farley, K. J. and F. M. M. Morel. 1986. Role of coagulation in sedimentation kinetics. Environ. Sci. Tech., *20,* 187–195.

Fleer, A. P. and M. P. Bacon. 1991. Updated determination of particulate and dissolved thorium-234, *in* Marine Particles: Analysis and Characterization, D. C. Hurd and D. W. Spencer, eds., Amer. Geophys. Union Monograph, *63,* 227–228.

Glibert, P. M., M. R. Dennett and J. C. Goldman. 1985. Inorganic carbon uptake by phytoplankton in Vineyard Sound, Massachusetts. II. Comparative primary productivity and nutritional status of winter and summer assemblages. J. Exp. Mar. Biol. Ecol., *86,* 101–118.

Glibert, P. M., J. C. Goldman and E. J. Carpenter. 1982. Seasonal variations in the utilization of ammonium and nitrate by phytoplankton in Vineyard Sound, Massachusetts, USA. Mar. Biol., *70,* 237–249.

Goldberg, E. D. 1954. Marine geochemistry. I. Chemical scavengers of the sea. J. Geol., *62,* 249–265.

Gschwend, P. M. and S. C. Wu. 1985. On the constancy of sediment-water partition coefficients of hydrophobic organic pollutants. Environ. Sci. Tech., *19,* 90–96.

Honeyman, B. D., L. S. Balistrieri and J. W. Murray. 1988. Oceanic trace metal scavenging: the importance of particle concentration. Deep-Sea Res., *35,* 227–246.

Honeyman, B. D. and P. H. Santschi. 1989. A Brownian-pumping model for oceanic trace metal scavenging: Evidence from Th isotopes. J. Mar. Res., *47,* 951–992.

—— 1991. Coupling adsorption and particle aggregation: laboratory studies of "colloid pumping" using ^{59}Fe-labelled hematite. Environ. Sci. Tech., *25,* 1739–1747.

—— 1992. The role of particles and colloids in the transport of radionuclides and trace metals in the oceans, *in* Environmental Particles, J. Buffle and H. P. van Leeuwen, eds., Lewis Publishers, *1,* 379–423.

Karl, D. M., G. A. Knauer and J. H. Martin. 1988. Downward flux of particulate organic matter in the ocean: a particle decomposition paradox. Nature, *332,* 438–441.

Kirchman, D. L., Y. Suzuki, C. Garside and H. W. Ducklow. 1991. High turnover rates of dissolved organic carbon during a spring phytoplankton bloom. Nature, *352,* 612–614.

Koike, I., S. Hara, K. Terauchi and K. Kogure. 1990. Role of sub-micrometre particles in the ocean. Nature, *345,* 242–243.

Longhurst, A. R., I. Koike, W. K. W. Li, J. Rodriguez, P. Dickie, P. Kepkay, F. Partensky, B. Bautista, J. Ruiz, M. Wells and D. F. Bird. 1992. Sub-micron particles in northwest Atlantic shelf water. Deep-Sea Res., *39,* 1–7.

Martin, W. R. and F. L. Sayles. 1987. Seasonal cycles of particle and solute transport processes in nearshore sediments: ^{222}Rn/^{226}Ra and ^{234}Th/^{238}U disequilibrium at a site in Buzzards Bay, MA. Geochim. Cosmochim. Acta, *51,* 927–943.

Journal of Marine Research

Minagawa, M. and S. Tsunogai. 1980. Removal of ^{234}Th from a coastal sea: Funka Bay, Japan. Earth Planet. Sci. Lett., *47*, 51–64.

Moore, R. M. and K. A. Hunter. 1985. Thorium adsorption in the ocean: reversibility and distribution amongst particle sizes. Geochim. Cosmochim. Acta., *49*, 2253–2257.

Moran, S. B. 1991. The application of cross-flow filtration to the collection of colloids and their associated trace metals in seawater, *in* Marine Particles: Analysis and Characterization, D. C. Hurd and D. W. Spencer, eds., Amer. Geophys. Union Monograph *63*, 275–280.

Moran, S. B. and K. O. Buesseler. 1992. Short residence time of colloids in the upper ocean estimated from ^{238}U-^{234}Th disequilibria. Nature, *359*, 221–223.

Moran, S. B. and R. M. Moore. 1989. The distribution of colloidal aluminum and organic carbon in coastal and open ocean waters off Nova Scotia. Geochim. Cosmochim. Acta, *53*, 2519–2527.

—— 1992. Kinetics of the removal of dissolved aluminum by diatoms in seawater: a comparison with thorium. Geochim. Cosmochim. Acta, *56*, 3365–3374.

Morel, F. M. M. and P. M. Gschwend. 1987. The role of colloids in the partitioning of solutes in natural waters, *in* Aquatic Surface Chemistry, W. Stumm, ed., Wiley, 405–422.

Murnane, R. J., J. L. Sarmiento and M. P. Bacon. 1990. Thorium isotopes, particle cycling models, and inverse calculations of model rate constants. J. Geophys. Res., *95*, 16,195–16,206.

Niven, S. E. H. and R. M. Moore. 1988. Effect of natural colloidal matter on the equilibrium adsorption of Th in seawater, *in* Radionuclides: A Tool for Oceanography, J. C. Guary *et al.,* eds., Elsevier, 111–120.

Nozaki, Y., Y. Horibe and H. Tsubota. 1981. The water column distributions of thorium isotopes in the western North Pacific. Earth Planet. Sci. Lett., *54*, 203–216.

Nozaki, Y., H. S. Yang and M. Yamada. 1987. Scavenging of thorium in the ocean. J. Geophys. Res., *92*, 772–778.

Santschi, P. H., Y.-H. Li and J. Bell. 1979. Natural radionuclides in the water of Narragansett Bay. Earth Planet. Sci. Lett., *45*, 201–213.

Smith, D. C., M. Simon, A. L. Alldredge and F. Azam. 1992. Intense hydrolytic enzyme activity on marine aggregates and implications for rapid particle dissolution. Nature, *359*, 139–142.

Strickland, J. D. H. and T. R. Parsons. 1972. A Practical Handbook of Seawater Analysis, 2nd Edition, Fisheries Research Board of Canada, Ottawa, 310 pp.

Stumm, W. 1977. Chemical interaction in particle separation. Environ. Sci. Tech., *11*, 1066–1070.

Tanaka, N., Y. Takeda and S. Tsunogai. 1983. Biological effect on removal of Th-234, Po-210 and Pb-210 from surface water in Funka Bay, Japan. Geochim. Cosmochim. Acta., *47*, 1783–1790.

Watson, S. W., T. J. Novitsky, H. L. Quinby and F. W. Valois. 1977. Determination of bacterial number and biomass in the marine environment. Appl. Environ. Microbiol., *33*, 940–946.

Wei, C.-L. and J. W. Murray. 1992. Temporal variations of ^{234}Th activity in the water column of Dabob Bay: particle scavenging. Limnol. Oceanogr., *37*, 296–314.

Wells, M. L. and E. D. Goldberg. 1991. Occurrence of small colloids in sea water. Nature, *353*, 342–344.